Optical Measurement of Millimeter-wave Antenna for Imaging Concealed Cracks on Concrete Surface

H. Togo[1], S. Mochizuki[1], S. Oka[2], I. Toyoda[3], N. Kukutsu[1], and Y. Kado[1]

[1]*NTT Microsystem Integration Laboratories*

3-1, Morinosato Wakamiya, Atsugi-shi, Kanagawa, 243-0198 Japan

togo@aecl.ntt.co.jp, mochi@aecl.ntt.co.jp, kukutsu.naoya@lab.ntt.co.jp, kado@aecl.ntt.co.jp

[2]*NTT Access Network Service Systems Laboratories*

1-7-1 Hanabatake, Tsukuba-city, Ibaraki, 305-0805 Japan

oka@ansl.ntt.co.jp

[3]*NTT Network Innovation Laboratories*

1-1 Hikari-no-oka, Yokosuka, Kanagawa, 239-0847 Japan

toyoda.ichihiko@lab.ntt.co.jp

***Abstract*— We have developed a handy near-field imaging system (Crack Scan) to nondestructive inspect decrepit concrete structures. In Crack Scan, 77-GHz band tapered slot antennas (TSAs) are arrayed to simultaneously detect MMWs scattered from surface cracks on the concrete covered with paint, wallpaper, and repair material. An optical electric-field sensor based on electro-optic effect characterizes the TSA to improve the spatial resolution of Crack Scan. Antenna measurements with the optical electric-field sensor demonstrated that our TSA with substrate cutting and corrugation provides high directivity. A measured near-field distribution indicates that directivity and polarization is degraded by an antenna electrode formed on each face of a substrate. Those results present useful guidelines to design the high directive antenna of Crack scan.**

I. Introduction

The hazard of decrepit concrete structures, such as expressways built long years ago, is becoming a serious problem. One of the most important aspects of assessing the durability of concrete structures is inspection for surface cracks. Though the allowed crack width slightly differs according to the criterion of each country, it is about 0.3-0.4 mm in dry air, and slightly less in humid air. Cracks in an exposed concrete surface can be detected by visual inspection. However, in buildings, the walls are often covered with paint, wallpaper, and repair material, making it difficult to detect surface cracks visually. To overcome this problem, we are investigating millimeter-wave (MMW) imaging to develop technology for detecting concrete surface cracks. MMWs can penetrate materials like cloth and plastic. Using this property, some imaging applications, such as security gates at airport and aviation monitoring systems, have been developed in recent years.

On the other hand, we have proposed the idea of employing the advantage of near-field imaging. Though the spatial resolution of quasi-optics MMW imaging systems, such as a security camera, is limited to several millimeters by the wavelength, the spatial resolution of our imaging system reaches the sub-millimeter order by capturing the dispersion of MMWs in the near field. Using this approach, we developed a nondestructive imaging tool called "Crack Scan" for detecting fine surface cracks of concrete structures by means of real-time scanning as shown [1], [2]. In Crack Scan, a few ten means of 77-GHz band antennas are stacked to simultaneously detect MMWs scattered from surface cracks as shown in Fig. 1. The spacing between each antenna should be close for high spatial resolution. The antennas should be highly directive to prevent interference with neighbouring antennas. Therefore, antenna measurement is important for optimizing antenna characteristics, such as a near-field pattern and directivity. In conventional measurement with metallic antennas and coaxial cables, an undesired scatter and the superimposition of noise is a concern. Electric field sensors with electro-optic (EO) crystals have recently attracted considerable attention as a possible means of solving these problems. Loh has demonstrated that using an optical sensor

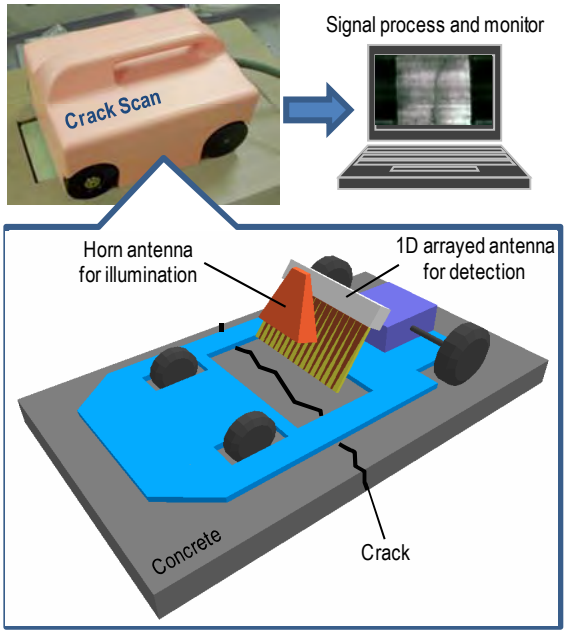

Fig. 1 Crack Scan and its configurations

as an EO transducer and replacing the coaxial cable by an optical fiber can suppress the undesired scatter in small antenna pattern testing in the frequency range of 2.4 to 2.5 GHz [3]. In the MMW region, the antenna mounted on the optical sensor may disturb the electric field due to its electrical coupling and scatter. To reduce the distribution, we have developed an optical sensor without any metal, such as an antenna, which can detect MMWs within a frequency range of 150 GHz [4].

This paper first describes a practical measurement system for characterizing MMW antennas with the optical sensor mounted on the fiber tip. It then describes the measurements of Crack Scan antenna for characterizing its directivity. The results are compared with the results of conventional measurement and electro-magnetic field simulations to discuss the potential of the optical antenna measurement system.

II. Optical Electric-Field Sensor

The configuration of the developed optical electric-field sensor is shown in Fig. 2 [5]. The sensor tip comprises an EO crystal with a dielectric reflector, a Faraday rotator (FR), a lens, a glass ferrule, and an optical fiber. The size of the EO crystal is 1 x 1 x 1 mm^3. The diameter of optical beam propagating in the EO crystal is 200 µm which determines the spatial resolution to detect the transverse electric field. The optical electric-field sensor is connected to a polarization controller through a 5-m long optical fiber, as shown in Fig. 3. Theoretically, the system should operate with stable sensitivity even if the optical fiber is extended to a length of 1 km. The measured antenna and the optical electric-field sensor are set in an anechoic chamber shielded electromagnetically, and the other instruments are located outside of the chamber.

A light source (10-GHz Tunable Picosecond Laser (MLLD-100)/ Alnair Laboratories Corporation) inputs an optical signal into the fiber and a photodetector receives the optical signal modulated with MMWs in the optical sensor. MMWs are detected with EO sampling technique [6]. The EO crystal acts as a harmonic mixer between the optical signal and the MMWs. MMWs are down-converted to replicas with the differential frequency of the optical signal and the MMWs. In the system, the light source generates the 2-ps duration pulse with a repetition frequency of 10 GHz and the differential frequency of 20 kHz, and the photodetector with an occupied bandwidth below 1 GHz filters out higher frequency components. Theoretically, this setup can detect the MMWs within a frequency of around 250 GHz.

MMW electric field is measured by scanning the optical electric-field sensor as shown in Fig. 4. The sensor is fixed in an acrylic case attached to an x-z transition stage with a scanning area of 20 x 20 cm^2 and a spatial resolution of 10 µm. The sensor tip can access the antenna surface with a spatial resolution of 50 µm in a direction along y-axis. A 77-GHz signal is input from the multiplier to the antenna via a metal base with a V-band waveguide. During scanning, the sensitivity of the optical electric-field senor is stable with a fluctuation of less than 0.5 dB.

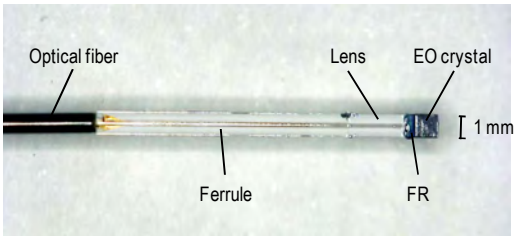

Fig. 2 Tip of optical electric-field sensor

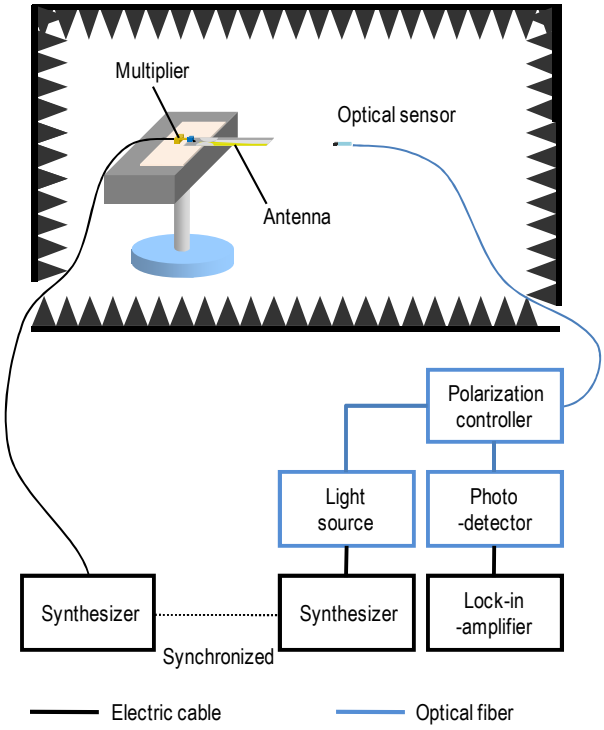

Fig. 3 Configuration of antenna measurement system with our optical electric-field sensor

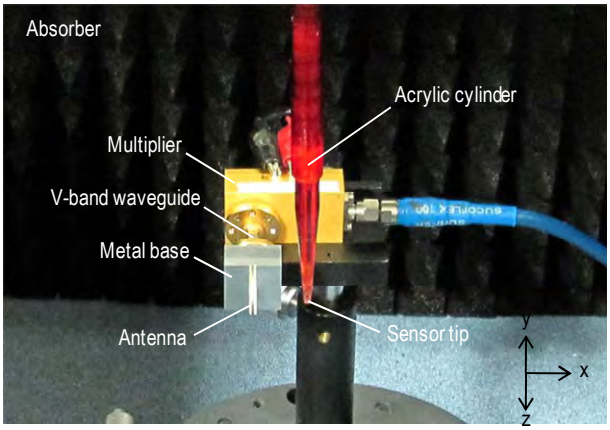

Fig. 4 2D near-field measurement setup with optical electric-field sensor

III. MMW Antenna Crack Scan

Figure 5 illustrates the configuration of the Crack Scan antenna, which is a tapered slot antenna (TSA) with substrate cutting and corrugation [7]. It was built by forming 5-mm thick Au film on both sides of an Al_2O_3 substrate with a relative dielectric constant of 8.1, loss tangent of 10^{-4}, and thickness of 0.1 mm. It consists of two parts: a coplanar waveguide (CPW)-to-slotline transition and a tapered slotline. It has a uniquely shaped substrate below the slotline formed by substrate cutting. This shape produces a difference in radiation patterns in the E- and H-planes. Corrugation is used on both sides of the tapered slotlines to reduce sidelobe levels. We computed the radiation patterns in the E- and H-planes of the developed antenna and those of a TSA without substrate cutting and corrugation. The developed antenna has a beamwidth of 60 degree for the E and H-plane, which is narrower than those other TSAs. This difference in the radiation patterns is mainly a result of removing the substrate below the tapered slotline. The electromagnetic energy flowing from the feed point to the aperture of the developed TSA is highly concentrated in the substrate below the tapered slotline. When the substrate below the slotline is removed, the energy spreads in the direction of the H-plane; it cannot spread in the direction of the E-plane due to the limited slotline width. Calculation of the antenna gain shows that the corrugation and substrate cutting increase the gain from around 5 to 14.2 dBi.

IV. MMW Antenna Measurement

The antenna patterns of the developed TSA measured with a standard gain horn antenna and the optical electric-field sensor are shown with the simulated pattern in Fig. 6. The patterns measured with the optical sensor agree with the simulation better than those measured with the horn antenna. In the E-plane, the optical sensor suppresses the increase of sidelobes, which cause multiple reflections between the horn antenna and the metal base supporting the TSA.

The intensity distributions of near field along x- and z-axis at the distance of 0.1 mm from an antenna surface are shown in Fig. 7 (b) and (c). The electric field along x-axis propagates symmetrically with respect to z-axis. The field along z-axis splits at the bottom of the slot and asymmetrically propagates because antenna electrode is formed on each side of the substrate, which degrades directivity and polarization. The phase distributions of near field along x- and z-axis at the distance of 0.1 mm from the antenna surface are shown in Fig. 8 (a) and (b). The phases of near field along x- and z-axis are different.

The intensity distributions of near field along x-axis on the plane at the distance of 0.1 and 5 mm from the antenna aperture are shown in Fig. 9 (a) and (b). The near-distribution is elliptical and the spread on y-axis is broader than that on x-axis. The distributions of near field at the distance of 0.1 and 5 mm from the antenna aperture on the white dot line in Fig. 9

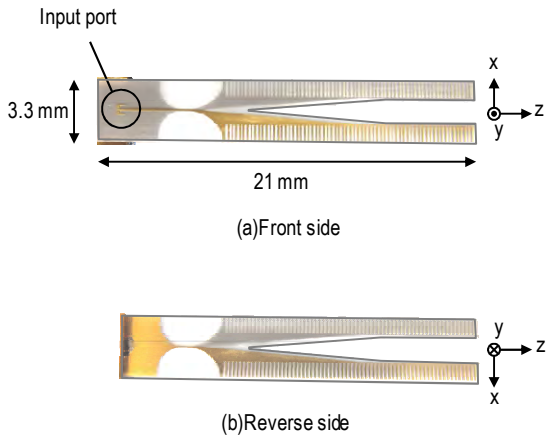

Fig. 5 77-GHz tapered slot antenna for Crack Scan

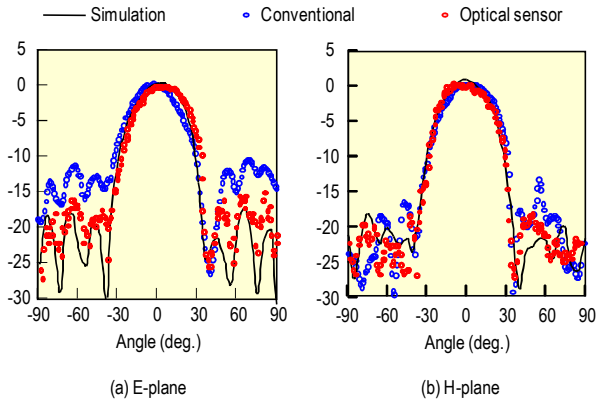

Fig. 6 Antenna pattern on E-plane (a) and H-plane (b)

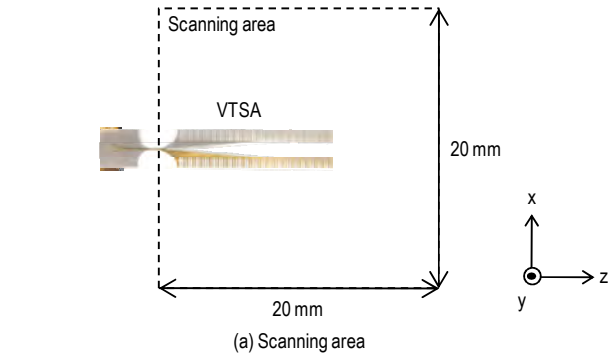

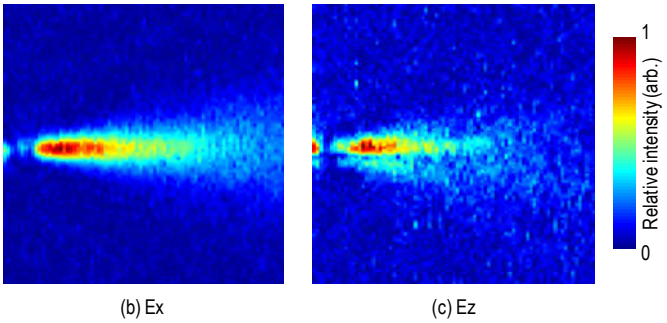

Fig. 7 Scanning area (a), intensity distributions of near field along x-axis (b) and z-axis (c)

are shown in Fig. 10 (a) and (b). The full width at half maximum of radiated electric field at 0.1 and 5 mm from the aperture are 4.5 and 7.5 mm, which determines the spatial resolution of Crack Scan. The spatial resolution at 5 mm from the aperture is evaluated to be two-thirds of that at 0.1 mm. This indicates that the antenna of Crack Scan should be positioned close to an imaging target to improve the spatial resolution.

V. Conclusions

Antenna measurements with an optical electric-field sensor demonstrated that our 77-GHz band TSA with substrate cutting and corrugation provides high directivity. These results indicate that the optical electric-field sensor is suitable for precise MMW antenna measurement. A measured near-field distribution indicates that directivity and polarization is degraded by an antenna electrode formed on each face of a substrate. With those results, we will develop high directive antennas to improve the spatial resolution of Crack Scan.

Acknowledgment

We would like to thank Dr. Sze Y. Set, Mr. K. Miyaji, Mr. M. Tojo, and Mr. K. Furuki of Alnair Laboratories Corporation for their useful and discussions in constructing the optical electric-field senor system, and Mr. T. Sugiyama of New Japan Radio Co. Ltd. for his advices in designing and manufacturing the TSA.

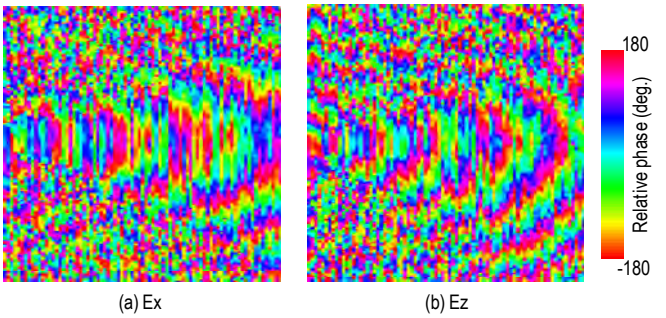

Fig. 8 Phase distributions of near field along x-axis (b) and z-axis (c)

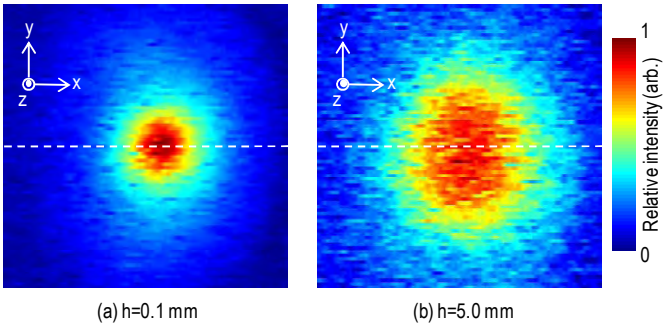

Fig. 9 Intensity distributions of near field along x-axis at 0 mm (a) and 5 mm from antenna aperture (b).

References

[1] S. Oka, H. Togo, and N. Kukutsu. "Latest trends in millimeter-wave imaging technology," *Progress in Electromagnetics Research Letters,* Vol. 1, pp. 197-204, 2008.

[2] S. Oka, S. Mochizuki, H. Togo, and N. Kukutsu, A neural network algorithm for detecting invisible concrete surface cracks in near-field millimetre-wave images," in Proceeding of *IEEE International Conference on System, Man and Cybernetics 2009 (SMC 2009)*, pp. 3801-3805, San Antonio, October 2009.

[3] T. H. Loh, M. Alexander, P. Miller, and T. Palmer, "Small antenna pattern testing-the antenna-to-range interface," *European Conference on Antennas and Propagation 2007(EUCAP 2007)*, pp. 1-6, Edinburgh, November 2007.

[4] H. Togo, A. Sasaki, A. Hirata, and T. Nagatsuma, "Characterization of millimeter-wave antenna using photonic measurement techniques," *Int. J. RF and Microwave CAS*, vol. 14, pp. 290-297, 2004.

[5] H. Togo, N. Kukutsu, N. Shimizu, and T. Nagatsuma, "Sensitivity-Stabilized Fiber-Mounted Electrooptic Probe for Electric Field Mapping," *Journal of Lightwave Technology*, Vol.26, No.15, pp. 2700-2705, 2008.

[6] A. Sasaki and T. Nagatsuma, "Millimeter-wave imaging using an Electrooptic detector as a harmonic mixer," *IEEE J. Sel. Top. Quantum Electron,* Vol. 6, pp. 735–740, 2000.

[7] S. Mochizuki, H. Togo, N. Kukutsu, T. Nagatzuma, "High-resolution SAR imaging system using tapered slot antenna with orthogonally anisotropic directivity, " *APACE 2007*, 4-6 December 2007, pp. 1-4.M. Wegmuller, J. P. von der Weid, P. Oberson, and N. Gisin, "High resolution fiber distributed measurements with coherent OFDR," in *Proc. ECOC'00*, 2000, paper 11.3.4, p. 109.

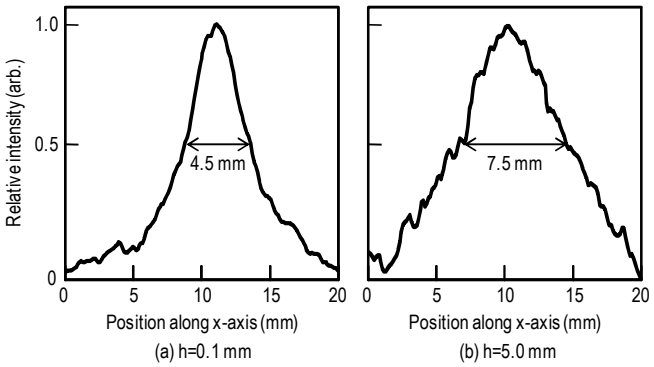

Fig. 10 Intensity distributions of near field along x-axis at 0 mm (a) and 5 mm from antenna aperture (b) on white dot lines in Fig. 9.